AMD-Vol. 151/PVP-Vol. 247, Symposium on Flow-Induced Vibration and Noise – Volume 7
ASME 1992

FLOW EXCITED ACOUSTIC RESONANCE IN A DEEP CAVITY: AN ANALYTICAL MODEL

William W. Durgin
Worcester Polytechnic Institute
Worcester, Massachusetts

Hans R. Graf
Sulzer Brothers Limited
Winterthur, Switzerland

ABSTRACT

Flow past the opening of a deep cavity can excite and sustain longitudinal acoustic modes resulting in large pressure fluctuations and loud tone generation. An analytic model of the interaction of the free stream with the acoustic flow field using concentrated vortices in the shear layer is proposed. The model includes a computation of the power transferred by the traveling vortices to the acoustic oscillation in the cavity. Experimentally measured values for the vortex convection velocity and phase are used to enable calculation of the ensuing oscillation amplititude and frequency ratio. The radiated acoustic power is calculated using the model and compared to that found from the measured velocity field.

Agreement between the model and experiments is found to be good for both the single and double vortex modes near resonance and for values of Ur above the single vortex mode. The single vortex mode resonance, the greatest oscillation amplititude, occurs at Ur = 3.2 with only a single vortex in the cavity opening. The double vortex mode resonance occurs at Ur = 1.5 with two vortices in the cavity opening simultaneously. In between the modes, the predicted power is too small probably resulting from difficulties in computing the generated acoustic power from the measured velocity field in this region.

NOMENCLATURE

A	area of cross section
b	span-wise dimension of cavity
c	speed of sound
d	depth of cavity
f	frequency of tone
f_n	natural frequency of the cavity
H	transfer function
k	wave number
L	stream-wise cavity dimension (= reference length)
m	summation index
Ma	Mach number $= \frac{U_\infty}{c}$
Pa	power of acoustic source
$\overline{Pa}$	average acoustic power
Pr	radiated power
Q	quality factor of resonator
r	frequency ratio f/f_n
r, θ	coordinates (leading edge is origin)
s	acoustic source (power per unit volume)
St	Strouhal number $= fL/U_\infty$
t	time
U_∞	free stream velocity (= reference velocity)
u_Γ	convective velocity of the vortex, divided by U_∞
U_r	reduced velocity $= U_\infty/f_n L$
$\vec{u}$	local flow velocity (x, v)
$\vec{v}$	acoustic particle velocity (v_x, v_y)
v	$= \frac{\partial h}{\partial t}$ = y-component of $\vec{v}$, averaged over a cross section of cavity
V	root -mean-square of acoustic velocity $\frac{v}{U_\infty}$ at y = 0
$\vec{w}$	$= \vec{u} - \vec{v}$ = velocity component of grazing flow
x, y	coordinates (leading edge is origin)
x_Γ, y_Γ	coordinates of concentrated vortex
Γ	circulation of vortex
ρ	fluid density

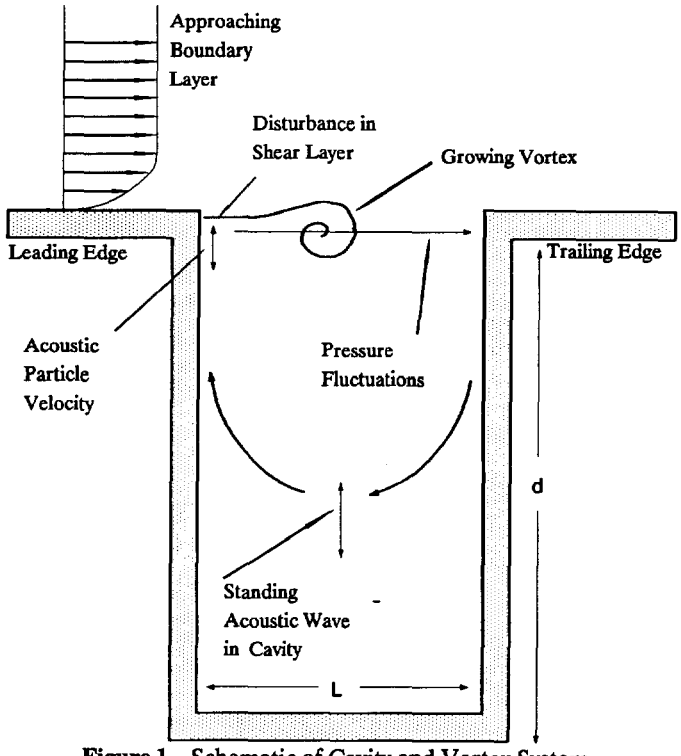

Figure 1. Schematic of Cavity and Vortex System

φ	phase of acoustic oscillation $= 2\pi ft$
φ_Γ	phase at vortex formation (x=0)
$\vec{\omega}$	vorticity
ξ	relative coordinate $= x - x_\Gamma$
η	relative coordinate $= y - y_\Gamma$

INTRODUCTION

Flow past a cavity can excite strong acoustic resonance. The unstable shear layer in the cavity mouth rolls up into large scales vortices which travel across the opening and excite acoustic oscillation, Figure 1. The oscillation, in turn, triggers the periodic formation of vortices. The overall gain in this feedback loop is a function of the reduced velocity, U_r. For the case of interest here, the longitudinal or depth acoustic modes predominate so that d is the appropriate acoustic length scale.

Plumblee et al (1) conducted subsonic and supersonic tests of flow past cavities and measured the frequency and amplititude of the response. For cavities with length greater than 2 or 3 times the size of the opening, they found excitation of the longitudinal mode. Analyses showed that the frequency excited corresponded to the natural frequency of the appropriate mode although significant buffet response was also present. East (2) conducted a series of experiments where the amplititude and frequency of the sound pressure at the bottom of a rectangular cavity were measured as a function of cavity geometry and free stream velocity. He found that tones were produced when the shear layer oscillation was amplified by a positive feedback loop involving the acoustic coupling between the shear layer pressure fluctuations and the cavity modes. East deduced that the convection velocity, u_Γ, of the disturbances in the shear layer was in the range 0.35...0.6 and tended to be lower for thick approaching boundary layers. Optimal acoustic coupling occured in two ranges of Strouhal number; S_t = 0.3...0.4 and S_t = 0.6...0.9.

Tam and Block (3) conducted experiments to determine the frequencies of discrete tones in rectangular cavities excited by a wide range of external flow Mach numbers. Their work concentrated on lateral modes as are associated with shallow cavities. A mathematical model was developed in which the shear layer switched into and out of the cavity thus driving the oscillation. They included a feedback mechanism in which the acoustic wave triggered the instability in the shear layer. Howe (4) develops a small perturbation model wherein the Kelvin-Helmholtz instability is excited in the shear layers associated with flow tangential to mesh screens. He argues that the Kutta condition at the upstream edge is a necessary condition for energy input to the oscillation. For deep cavaties, those with depth substantially greater than the dimension of the opening in the flow direction, Graf (5) has shown that the normal acoustic mode predominates and that large vorticies form in the shear layer. Velocity

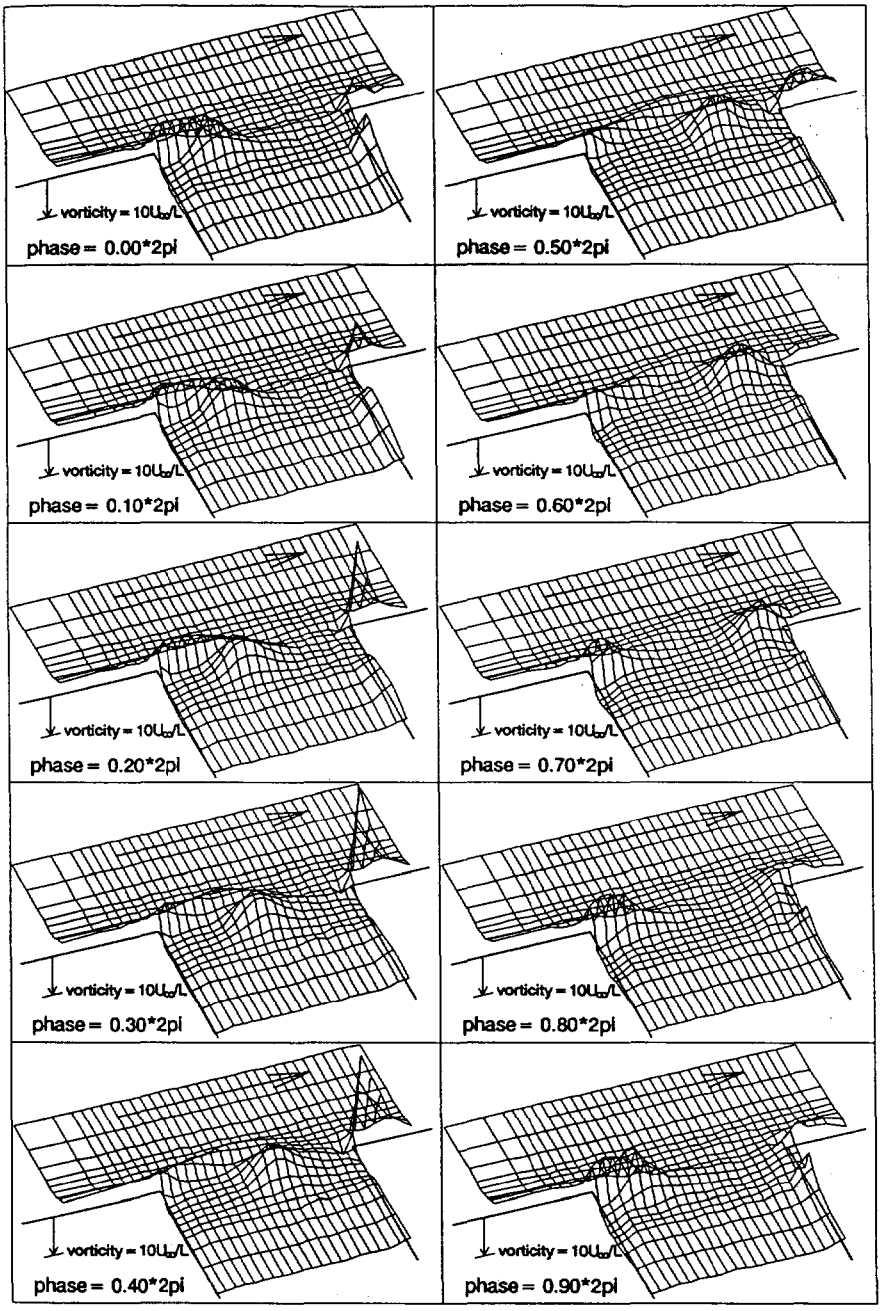

Figure 2. Vorticity Field for $U_r = 3.21$, $V = 0.069 \ldots 0.105$

measurements indicate that velocity perturbations near resonance are large.

The resonance at $U_r=3.2$ is so strong that the amplitude of the acoustic pressure in the cavity can exceed the dynamic pressure of the external flow, Graf (5). In this flow condition only one vortex populates the cavity opening and drives the oscillation to its maximum amplitude. A weaker resonance occurs at $U_r=1.5$ where two vortices are in the cavity opening simultaneously.

Since disturbances in the shear layer are large, linearized stability theory is not practical to model the excitation of the acoustic oscillation of the flow. Our experiments indicate that the vorticity which shed from the leading edge accumulates and forms discrete vortices. A model which describes the vorticity field with a few point vortices which traverse the cavity opening giving rise to a nonsteady pressure field is developed. The model, first described by Bruggerman (6), is modified and developed in light of our experimental findings.

Graf (5,7) reports detailed measurements of the velocity field in the vicinity of the opening of the cavity. The free stream flow was produced using a wind tunnel of .5 m dimension fitted with a cavity of L=6.5 cm. Velocity measurements were made using LDA. From these measurements the vorticity field, Figure 2, was computed. Additionally, the location of the vortex cores as a functions of the phase of the oscillation cycle were determined and are shown in Figure 3. These data form the basis for an analytical model of the acoustic resonance. It can be shown, Graf (5), that the acoustic source strength can be calculated as

$$s=\rho\left[\vec{v}\cdot\frac{\partial\vec{w}}{\partial t}+\vec{v}\cdot\nabla\left(\frac{|\vec{w}|^2}{2}+\vec{w}\cdot\vec{v}\right)+\vec{v}\cdot\vec{\omega}\times\vec{w}\right] \quad (1)$$

where $\vec{w}=\vec{u}-\vec{v}$ and $\vec{w}$ is the velocity while $\vec{v}$ is the acoustic velocity.

Concentrated Vortex Model

In the simplified model considered here, one point vortex forms in each acoustic cycle and travels across the cavity opening at a constant velocity $u_\Gamma \cdot U_\infty$. Vorticity is shed from the leading edge at a constant rate $d\Gamma/dt=-1/2\,U_\infty^2$. This vorticity is added to the circulation of the vortex, although the vortex is now at a distance x_Γ downstream of the leading edge Figure 4. After one acoustic cycle the next vortex forms, and the vorticity accumulates in this new vortex. Consequently, the circulation of the original vortex remains constant $\Gamma=-1/2\,U_\infty^2/f$ until it reaches the downstream edge. For the purpose of this model, the vortex is subsequently ignored. In reality, on impingment some vorticity is swept downstream into the cavity while some is swept downstream in the external flow.

Assuming the vortex forms at phase $\varphi=\varphi_\Gamma$ at the leading edge and travels with constant velocity $u_\Gamma \cdot U_\infty$, the position of the vortex is given by Equation 2.

$$x_\Gamma=\frac{u_\Gamma}{St}\frac{\varphi-\varphi_\Gamma}{2\pi}\cdot L \quad (2)$$

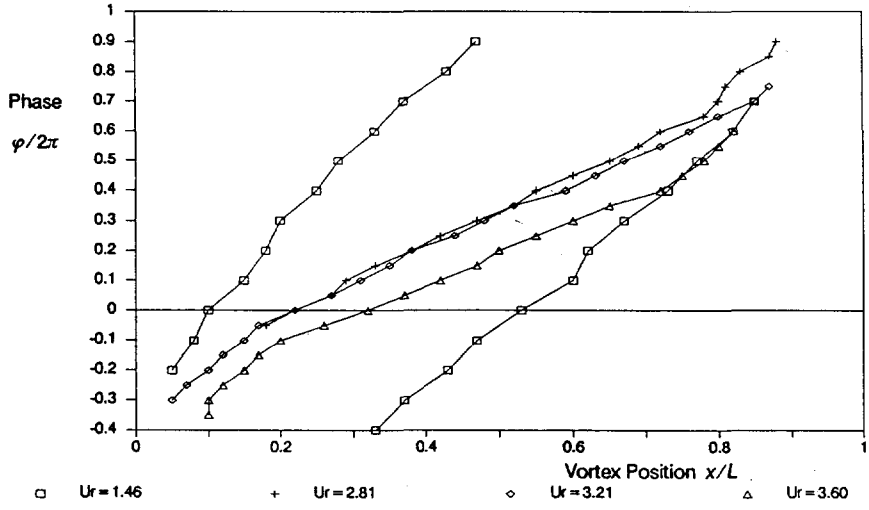

Figure 3. x-Location of the Vortex in the Cavity Opening as a function of the Phase in the Acoustic Cycle

The circulation increases during one cycle and then remains constant:

during first cycle:

$$\varphi-\varphi_\Gamma\le 2\pi \qquad \Gamma=-\frac{1}{2}\frac{\varphi-\varphi_\Gamma}{2\pi}\frac{1}{St}\cdot U_\infty L \quad (3a)$$

later:

$$\varphi-\varphi_\Gamma>2\pi \qquad \Gamma = -\frac{1}{2}\frac{1}{St}\cdot U_\infty L \tag{3b}$$

The flow field around this vortex can be described as the superposition of a uniform parallel flow and the point vortex itself. According to the vorticity transport equation, a free point vortex always moves with the fluid; therefore, the velocity of the parallel flow must be $u_\Gamma \cdot U_\infty$. Equation 4 describes the velocity field resulting from the superposition of the parallel flow and the velocity induced by the point vortex.

$$\vec{u} = \begin{Bmatrix} u_\Gamma \cdot U_\infty \\ 0 \end{Bmatrix} + \frac{\Gamma}{2\pi\left(\xi^2+\eta^2\right)} \cdot \begin{Bmatrix} -\eta \\ \xi \end{Bmatrix} \tag{4}$$

where $\xi=x-x_\Gamma$ and $\eta=y-y_\Gamma$ are the coordinates relative to the vortex core.

In this simplified model it is assumed that the acoustic particle velocity into and out of the cavity is in y-direction and uniform across the opening of the cavity.

$$\vec{v} = \begin{Bmatrix} v_x \\ v_y \end{Bmatrix} = \begin{Bmatrix} 0 \\ -\sqrt{2}V e^{i\varphi} \cdot U_\infty \end{Bmatrix} \tag{5}$$

Power Transferred to Oscillation

The power P_a transferred to the acoustic oscillation can now be computed by integrating over the area of the cavity mouth.

$$P_a = -b\cdot\rho\frac{\partial}{\partial t}\int\int \vec{v}\cdot(\vec{u}-\vec{v})\,dx\,dy - b\cdot\frac{\rho}{2}\int\int \vec{v}\cdot\nabla\left(|\vec{u}|^2-|\vec{v}|^2\right)dx\,dy - b\cdot\rho\sum_m \vec{v}_m\cdot\left(\vec{\Gamma}_m\times\vec{u}_m\right) \tag{6}$$

The summation includes all point vortices currently in the cavity opening. The integral of the first term in Equation 6 yields zero.The second term in Equation 6 can be evaluated for a single point vortex in an infinite parallel flow. The expressions 4 and 5 are substituted for $\vec{u}$ and $\vec{v}$ respectively.

$$|\vec{u}|^2-|\vec{v}|^2 = \frac{(\Gamma/2\pi)^2 - u_\Gamma U_\infty \eta\Gamma/\pi}{\xi^2+\eta^2} + \left(u_\Gamma U_\infty\right)^2 - v_y^2 \tag{7}$$

The integrand can be determined by taking the derivative of Equation 7 with respect to y (or η).

$$\vec{v}\cdot\nabla\left(|\vec{u}|-|\vec{v}|\right) = v_y\cdot\frac{\partial}{\partial\eta}\left(|\vec{u}|-|\vec{v}|\right) = v_y\cdot\frac{-2\eta\left(\Gamma/2\pi\right)^2 + \left(2\eta^2-\xi^2-\eta^2\right)u_\Gamma U_\infty\Gamma/\pi}{\left(\xi^2+\eta^2\right)^2} \tag{8}$$

This expression is now integrated over the infinite plane. Polar coordinates r and θ are used in place of ξ and η.

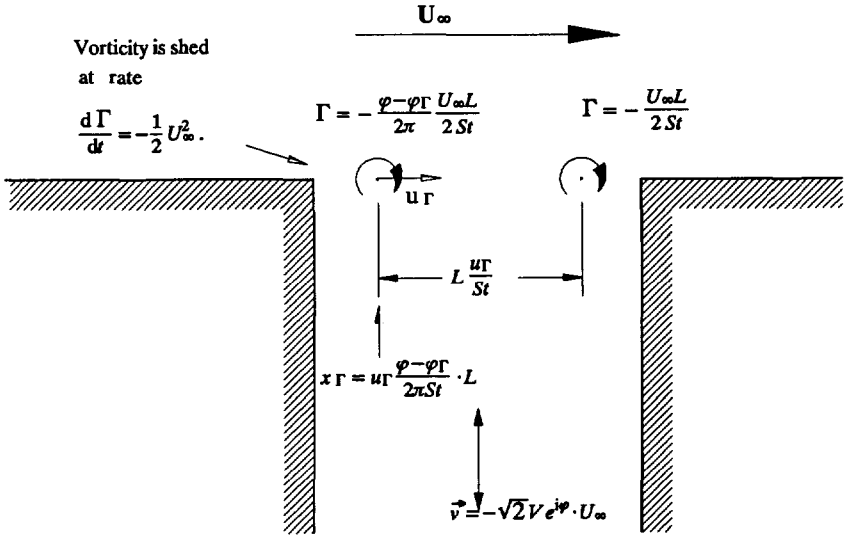

Figure 4. Point Vortices of the Concentrated Vortex Model

$$\int\int \vec{v}\cdot\nabla\left(|\vec{u}|-|\vec{v}|\right)\mathrm{d}x\,\mathrm{d}y$$

$$= \int_0^{\infty}\int_0^{2\pi} v_y \cdot \frac{-2r\sin\theta\left(\Gamma/2\pi\right)^2}{r^4} + \frac{\left(r^2\sin^2\theta - r^2\cos^2\theta\right)u_\Gamma U_\infty \Gamma/\pi}{r^4} r\,\mathrm{d}\theta\,\mathrm{d}r$$

$$= v_y \int_0^{\infty}\left[-\frac{2\left(\Gamma/2\pi\right)^2}{r}\int_0^{2\pi}\sin\theta\,\mathrm{d}\theta + \frac{u_\Gamma U_\infty \Gamma}{\pi}\int_0^{2\pi}\left(\sin^2\theta-\cos^2\theta\right)\mathrm{d}\theta\right]\frac{1}{r}\mathrm{d}r$$

$$= v_y \int_0^{\infty}\left[\,0 + \frac{u_\Gamma U_\infty \Gamma}{\pi}(\pi-\pi)\right]\frac{1}{r}\mathrm{d}r = 0 \qquad (9)$$

This shows that the second term in Equation 6 yields zero if the flow field consists of a point vortex in parallel flow. In the actual flow, however, the vorticity has a more continuous distribution; the flow field is therefore much more complex. In this case the second term in Equation 9 will in general not vanish. (Simple superposition of the flow fields does not apply because of the nonlinear properties of the equations.)

Even when the vorticity is concentrated in a point vortex, the second term in Equation 6 may not be exactly zero since the boundary conditions at the walls can disturb the ideal flow field. However, these effects are here neglected for simplicity, and only the third term remains in Equation 6.

Average Acoustic Power

The average power $\bar{P}_a$ transferred to the acoustic oscillation is determined by integrating the instantaneous power over one cycle.

If the Strouhal number is high enough ($St \geq u_\Gamma$), the next vortex forms before the previous one reaches the trailing edge. Therefore, one or more vortices are in the opening of the cavity at all times. The average power must include the contribution of all of these vortices.

$$\bar{P}_a = -b\cdot\rho\frac{1}{2\pi}\left(\int_{\varphi_\Gamma}^{2\pi+\varphi_\Gamma} v_y\,\Gamma(\varphi)\,u_\Gamma U_\infty\,\mathrm{d}\varphi + \int_{2\pi+\varphi_\Gamma}^{\frac{2\pi St}{u_\Gamma}+\varphi_\Gamma} v_y\,\Gamma(\varphi)\,u_\Gamma U_\infty\,\mathrm{d}\varphi\right)$$

$$= -bL\frac{\varrho}{2}U_\infty^3\frac{\sqrt{2}V}{2\pi}\frac{u_\Gamma}{St}\left(\int_{\varphi_\Gamma}^{2\pi+\varphi_\Gamma}\frac{(\varphi-\varphi_\Gamma)}{2\pi}e^{i\varphi}\,\mathrm{d}\varphi + \int_{2\pi+\varphi_\Gamma}^{\frac{2\pi St}{u_\Gamma}+\varphi_\Gamma} e^{i\varphi}\mathrm{d}\varphi\right) \qquad (10)$$

This expression can be simplified and written in dimensionless form

$$\frac{\bar{P}_a}{b\,L\,\rho/2U_\infty^3} = \frac{\sqrt{2}}{2\pi}V\frac{u_\Gamma}{St}\,e^{\,i\left(\frac{2\pi\,St}{u_\Gamma}+\frac{\pi}{2}+\varphi_\Gamma\right)} \qquad (11)$$

The real part of $\bar{P}_a$ is the average power transferred from the flow to the acoustic oscillation; the imaginary part corresponds to the reactive power and is related to the phase difference between v and $\sum\Gamma\cdot u_\Gamma$.

If a vortex requires less than one period to travel to the trailing edge, no vortex is in the cavity mouth for the rest of the cycle and the average power is given by

$$\bar{P}_a = -\rho b\frac{1}{2\pi}\int_{\varphi_\Gamma}^{\frac{2\pi\,St}{u_\Gamma}+\varphi_\Gamma} v\,\Gamma(\varphi)\,u_\Gamma U_\infty\,\mathrm{d}\varphi$$

$$= -\frac{\rho bL}{4\pi St}\sqrt{2}V U_\infty^3 u_\Gamma\int_{\varphi_\Gamma}^{\frac{2\pi f}{u_\Gamma}+\varphi_\Gamma}\frac{(\varphi-\varphi_\Gamma)}{2\pi}e^{i\varphi}\,\mathrm{d}\varphi \qquad (12)$$

which can be simplified to

$$\frac{\bar{P}_a}{b\,L\,\rho/2U_\infty^3} = \frac{\sqrt{2}}{2\pi}V\frac{u_\Gamma}{St}e^{i\varphi_\Gamma}\left[\left(i\frac{St}{u_\Gamma}-\frac{1}{2\pi}\right)e^{i\frac{2\pi St}{u_\Gamma}}+\frac{1}{2\pi}\right] \qquad (13)$$

For steady state oscillation the sum of radiated power P_r and attenuation in the cavity must be equal to the real part of $\bar{P}_a$, the acoustic power generated by the vortices. As Graf (5) shows, the power dissipated by attenuation in the cavity is small compared to P_r and

can be neglected. The radiated power increases proportional to V^2. The power $\bar{P}_a$ generated by the vortices, on the other hand, is proportional to V. The radiated power and the generated power are in equilibrium if

$$V^2 \frac{1}{Ma} \frac{k^2 A}{\pi} = \mathrm{Re}\left(\frac{\bar{P}_a}{b\, L\, \rho/2 U_\infty^3} \right) \tag{14}$$

to the acoustic oscillation has several peaks. The maximum at $1/St \approx 3.2$ coincides with resonance in the single vortex mode and $1/St \approx 1.6$ corresponds to the oscillation in the double vortex mode. The peaks at lower values of $1/St$ are pertinent to modes with more than two vortices in the cavity opening. In the experiments these modes were weak and could not be detected. When the average power is negative, energy is transferred from the acoustic mode to the flow, and the acoustic oscillation is actively damped.

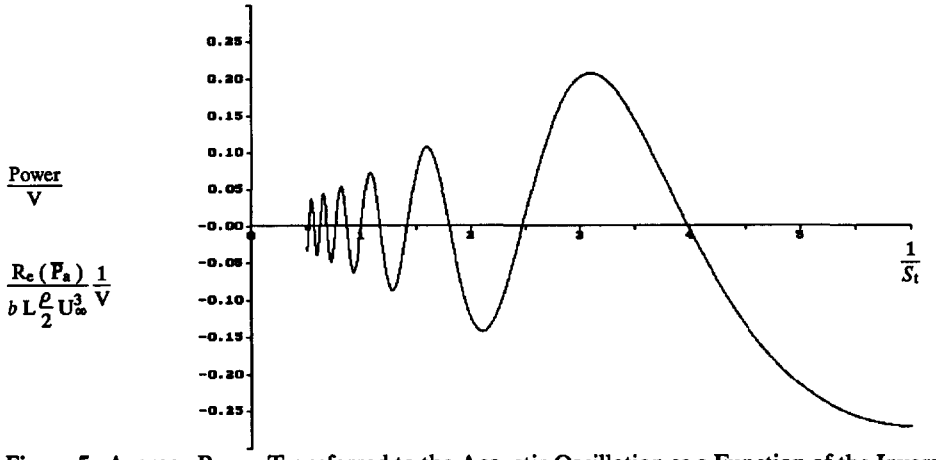

Figure 5. Average Power Transferred to the Acoustic Oscillation as a Function of the Inverse of the Strouhal Number; $u_\Gamma = 0.3$, $\varphi_\Gamma = -0.35 \cdot 2\pi$

Implementation of the Analytical Model

The values of vortex convection speed u_Γ, and the phase in the acoustic cycle φ_Γ, are selected based on the experimental data shown in Figure 3 : $u_\Gamma \approx 0.3$, $\varphi_\Gamma \approx -0.35 \cdot 2\pi$. The acoustic power generated by the vortices can now be computed as a function of the Strouhal number and the acoustic amplitude. The results are plotted in Figure 5 . The power transferred

Figure 6 shows the amplitude and frequency ratio of the oscillation obtained with the analytical model. The amplitude was computed based on the energy balance described by Equation 14 .

$$V = \mathrm{Re}\left(\frac{\bar{P}_a}{V \cdot b\, L\, \rho/2 U_\infty^3} \right) \cdot \frac{\pi\, Ma}{k^2 A} \tag{15}$$

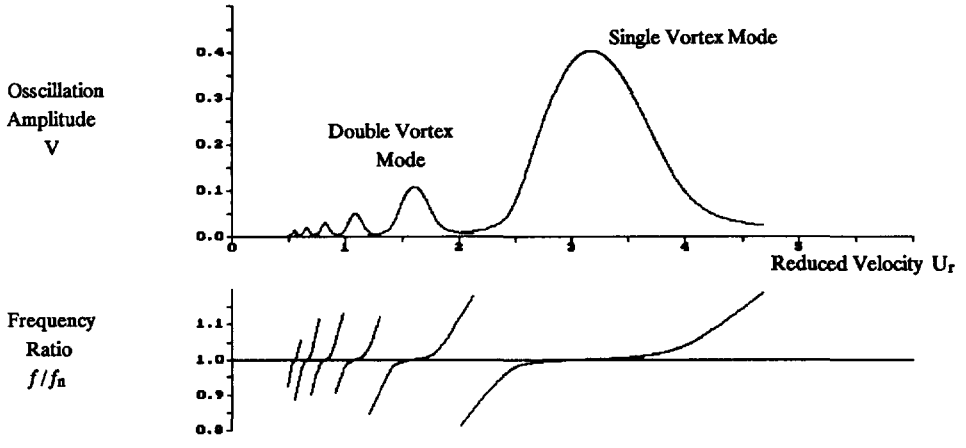

Figure 6. Amplitude and Frequency Ratio as a function of the Reduced Velocity Obtained with the Concentrated Vortex Model; $u_\Gamma = 0.3$, $\varphi_\Gamma = -0.35 \cdot 2\pi$, $Q = 80$

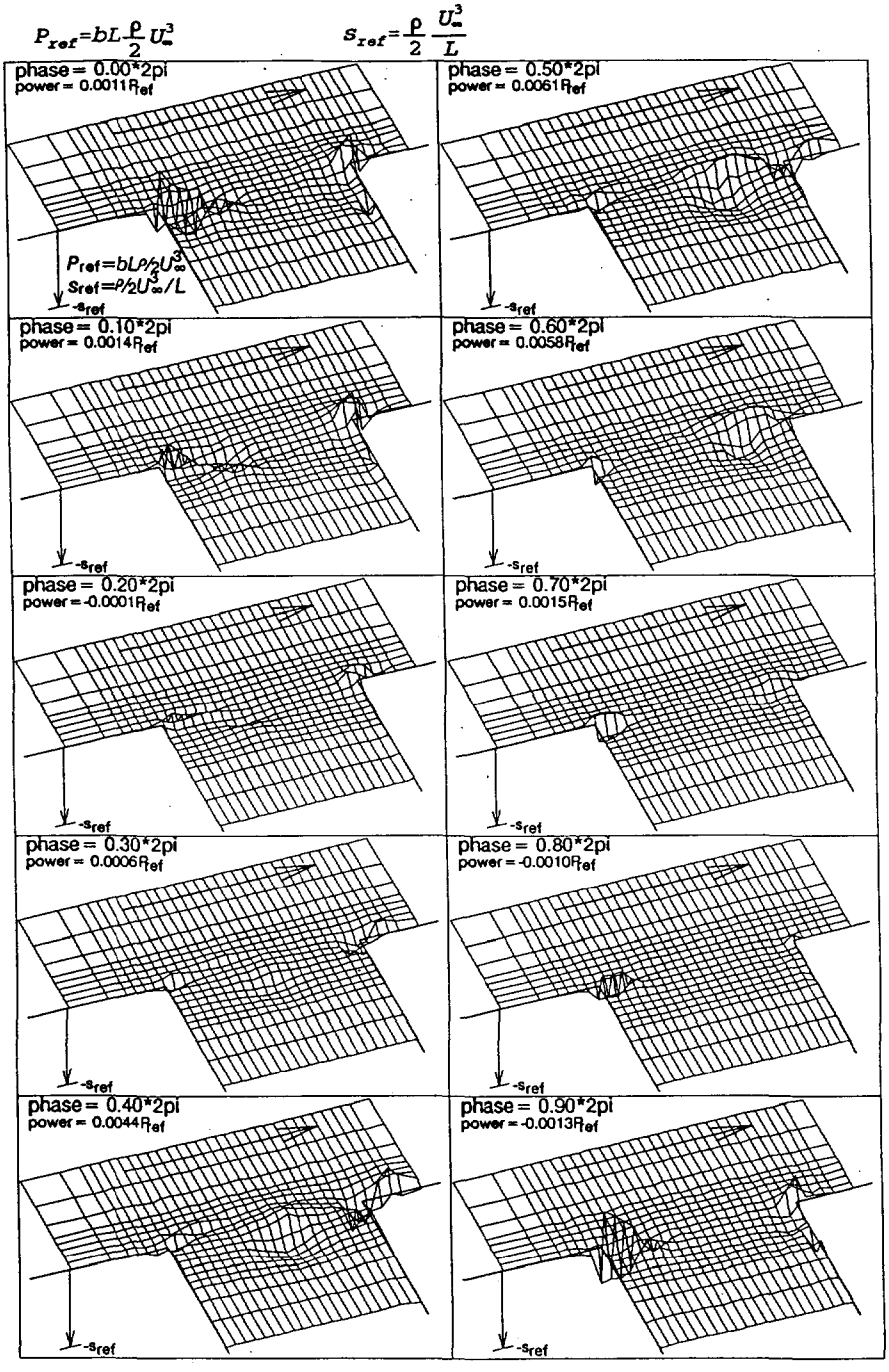

Figure 7. Acoustic Power Density s for U_r = 3.21, V = 0.069

The frequency ratio was determined by the following method involving the dynamic properties of the resonator. The argument of the complex power $\bar{P}_a$ is the phase difference between the pressure which excites the oscillation (driving force) and the acoustic velocity into and out of the cavity. This phase difference must be identical to the argument of the transfer function H which describes the dynamic behavior of the acoustic resonator. The resonator is here modeled as a harmonic oscillator with the velocity transfer function

$$H = \frac{\text{velocity } v \text{ (complex)}}{\text{driving force}} = Const \cdot \frac{ir}{1 + \frac{1}{Q} ir - r^2} \tag{16}$$

where $r = f/f_n$. The frequency ratio can now be determined by setting the arguments of $\bar{P}_a$ and H equal.

$$\arg \bar{P}_a \equiv \arctan\left(\frac{\mathrm{Im}\,\bar{P}_a}{\mathrm{Re}\,\bar{P}_a}\right) = \arg H \equiv \arctan\left(\frac{Q(1-r^2)}{r}\right) \tag{17}$$

This leads to a quadratic equation for r, which can easily be solved.

$$r^2 + r\frac{1}{Q}\frac{\mathrm{Im}\,\bar{P}_a}{\mathrm{Re}\,\bar{P}_a} - 1 = 0 \tag{18}$$

Qualitatively, the results match the experiments: the resonance peaks for the single and double vortex modes occur approximately at the correct reduced velocity. The amplitude in the double vortex mode is considerably lower than in the single vortex mode. The frequency ratio increases slightly as the reduced velocity passes through the resonance condition. Similar results were found experimentally by Panton (8) in studying Helmholtz resonator excitation coupled to exterior grazing flow with various orifices.

However, the predicted amplitude is approximately 4 times too high. In the actual flow the vorticity is not concentrated in a point vortex, but is more spread out in a "vorticity hill" Figure 2. Bruggeman 6 showed that a more distributed vorticity field reduces the intensity of the excitation considerably.

Acoustic Source of the Measured Flow

The acoustic power generated by the vortical flow in the shear layer can be computed based on the measured velocity field. The strength of the acoustic source s is evaluated according to Equation 1 . The vorticity distribution and the gradient of the dynamic pressure are determined by numerical differentiation.

In Figure 7 the distribution of s is plotted for resonance in the single vortex mode. Exchange of energy between the flow and the acoustic mode takes place primarily in the regions with high vorticity. When

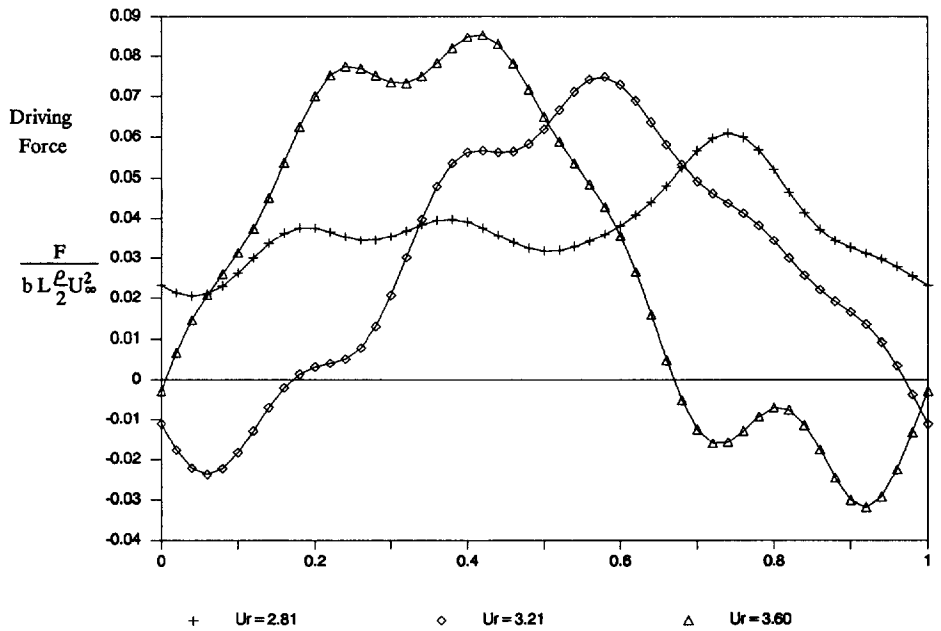

Figure 8. Driving Force as a Function of the Phase in the Acoustic Cycle; Data Computed Based on the Velocity Measurements

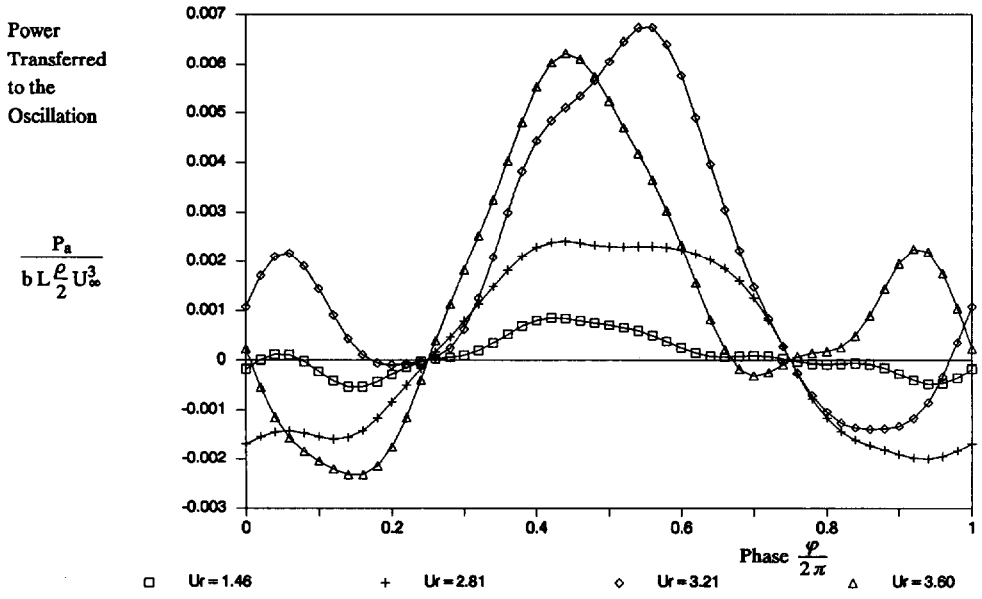

Figure 9. Power Transfer Between the Flow in the Shear Layer and the Acoustic Oscillation; Data Computed Based on the Velocity Measurements

air starts flowing into the cavity at $\varphi = 0.8...0.9 \cdot 2\pi$, s has a negative value directly downstream of the leading edge. This indicates that energy is transferred from the acoustic oscillation to the shear flow. A short distance further down in the cavity, some energy is transferred from the flow back to the acoustic oscillation. The intense exchange of energy at this location seems to be related to the process by which the acoustic flow induces a disturbance in the shear layer. Subsequently, this disturbance rolls up into the large scale vortex. The spatial resolution of the measurements near the leading edge is not high enough to allow for a more detailed analysis.

The driving force F, which excites the acoustic oscillation, is defined as the power $\bar{P}_a$ divided by the acoustic velocity v. In Figure 8 the driving force is plotted as a function of the phase. The curves for the three flow conditions are computed from the measured velocity data; only the single vortex mode is considered here. The phase where the driving force is maximum shifts from $\varphi \approx 0.75 \cdot 2\pi$ for $U_r = 2.81$ (below resonance) to $\varphi \approx 0.4 \cdot 2\pi$ for $U_r = 3.6$ (above resonance). This phenomenon is well known from the theory of the spring-mass oscillator (9). At resonance ($U_r = 3.2$) the peak of the driving force occurs at $\varphi / 2\pi \approx 0.5$. Since the velocity out of the cavity is also maximum at this phase, the power transfer to the oscillation is optimum at resonance. For excitation above or below resonance, the peak of the driving force does not coincide with the peak of the velocity, and the transfer of energy is therefore reduced. The same mechanism plays in a simple spring-mass oscillator.

Figure 9 shows the rate of energy transfer computed from the velocity measurements. Most of the

Table I. Average Power Transferred to the Acoustic Oscillation

U_r	V	$\frac{\bar{P}_a}{b L \rho/2 U_\infty^3}$	$\frac{P_r}{b L \rho/2 U_\infty^3}$
1.46	0.013	0.000092	0.00018
2.81	0.051	0.00018	0.0014
3.21	0.069	0.0018	0.0023
3.60	0.057	0.0013	0.0014

acoustic energy is generated between $\varphi/2\pi=0.25$ and $\varphi/2\pi=0.75$, when air is flowing out of the cavity. During this part of the acoustic cycle the vortex is fully developed and is traveling across the cavity opening towards the downstream edge. During the first and last quarters of the cycle, when air is flowing into the cavity, the instantaneous power P_a is negative at times, indicating that energy is transferred from the acoustic oscillation back to the shear flow.

The average power $\bar{P}_a$ generated by the moving vortices and the radiated acoustic power are listed in Table I for the four flow conditions investigated experimentally. Above resonance in the single vortex mode (U_r=3.6), the acoustic energy generated by the vortices agrees very well with the energy radiated from the orifice. At resonance in the double and single vortex mode ($U_r=1.5$ and $U_r=3.2$), the computed power produced by the vortices is somewhat smaller than the radiated power, but they are still in the same range. For $U_r=2.81$ the predicted power generated by the vortices is about 8 times too small. This indicates that it is difficult to compute the generated acoustic power from the measured velocity field. Since the experimental data must be differentiated numerically, very precise and detailed measurements are necessary in order to obtain accurate results.

REFERENCES

(1) Plumblee, H.E., Gibson, J.S. and Lassiter, L.W., " A Theoretical and Experimental Investigation of the Acoustical Response of Cavities in Aerodynamic Flow," WADD TR-61-75, March 1962, A.R.C. 24652, Mar. 1963.

(2) East, L.F., "Aerodynamically Induced Resonance in Rectangular Cavities," *J. Sound and Vibration*, Vol. 3, No. 3, 1966, pp. 277-287.

(3) Tam, C.K.W. and Block, P.J.W., "On the Tones And Pressure Oscillations Induced By Flow over Rectangular Cavities," *J. Fluid Mechanics*, vol 89, 1978, pp. 373-399.

(4) Howe, M.S., "The Influence of Mean Shear on Unsteady Aperature Flow, with Application to Acoustical Diffraction and Self-sustained Cavity Oscillations," *J. Fluid Mechanics*, 109, 1981, pp. 125-146.

(5) Graf, H.R., 1989, "Experimental and Computational Investigation of the Flow Excited Acoustic Resonance in an Deep Cavity," Ph.D. Dissertation, Worcester Polytechnic Institute, Worcester, MA.

(6) Bruggerman, J.C., " Flow Induced Pulsations in Pipe Systems, " Ph.D. Dissertation, Technical University Eindhoven, Netherlands.

(7) Graf, H.R., and W.W. Durgin, "Measurement of the Nonsteady FlowField in the Openings of a Resonating Cavity Excited by Grazing Flow," *Proceedings, International Symposium on Nonsteady Fluid Dynamics,* J.A. Miller and D.P. Telionis ed.,, ASME, 1990.

(8) Panton, R.L., "Effect of Orifice Geometry on Helmholtz Resonator Excitation by Grazing Flow," *AIAA Journal*,v. 28, n. 1, pp. 60-65, January 1990.

(9) Vierch, R.K., Vibration Analysis, 2nd ed. New York, Harper and Row, 1979.